

# $\beta$ -Carotene Radical Cation Addition to Green Tea Polyphenols. Mechanism of Antioxidant Antagonism in Peroxidizing Liposomes

Lin-Lin Song,<sup>†</sup> Ran Liang,<sup>\*,†</sup> Dan-Dan Li,<sup>†</sup> Ya-Dong Xing,<sup>†</sup> Rui-Min Han,<sup>†</sup> Jian-Ping Zhang,<sup>†</sup> and Leif H. Skibsted<sup>‡</sup>

<sup>†</sup>Department of Chemistry, Renmin University of China, Beijing 100872, China

<sup>‡</sup>Food Chemistry, Department of Food Science, Faculty of Life Sciences, University of Copenhagen, Rolighedsvej 30, DK-1058 Frederiksberg C, Denmark

**S** Supporting Information

**ABSTRACT:** Green tea polyphenols, (–)-epicatechin (EC), (–)-epigallocatechin (EGC), (–)-epicatechin gallate (ECG), and (–)-epigallocatechin gallate (EGCG), all showed antioxidative effect in liposomes for lipid oxidation initiated in the lipid phase (antioxidant efficiency EC > EGCG > ECG > EGC) or in the aqueous phase (EC  $\gg$  EGC > EGCG > ECG) as monitored by the formation of conjugated dienes. For initiation in the lipid phase,  $\beta$ -carotene, itself active as an antioxidant, showed antagonism with the polyphenols (EC > ECG > EGCG > EGC). The Trolox equivalent antioxidant capacity (TEAC EGC > EGCG > ECG > EC) correlates with the lowest phenol O–H bond dissociation enthalpy (BDE) as calculated by density functional theory (DFT). Surface-enhanced Raman spectroscopy (SERS) was used to assess the reducing power of the phenolic hydroxyls in corroboration with DFT calculations. For homogeneous (1:9 v/v methanol/chloroform) solution, the  $\beta$ -carotene radical cation reacted readily with each of the polyphenol monoanions (but not with the neutral polyphenols) with a rate approaching the diffusion limit for EC as studied by laser flash photolysis at 25 °C monitoring the radical cation at 950 nm. The rate constant did not correlate with polyphenol HOMO/LUMO energy gap (DFT calculations), and  $\beta$ -carotene was not regenerated by an electron transfer reaction (monitored at 500 nm). It is suggested that the  $\beta$ -carotene radical cation is rather reacting with the tea polyphenols through addition, as further evidenced by steady-state absorption spectroscopy and liquid chromatography–mass spectroscopy (LC-MS), in effect preventing regeneration of  $\beta$ -carotene as an active lipid phase antioxidant and leading to the observed antagonism.

**KEYWORDS:** catechin, green tea,  $\beta$ -carotene, antioxidant interaction

## INTRODUCTION

Fresh tea leaves contain up to 30% dry weight polyphenols, of which the catechins (–)-epicatechin (EC), (–)-epigallocatechin (EGC), (–)-epicatechin gallate (ECG), and (–)-epigallocatechin gallate (EGCG), as shown in Figure 1, are considered to be most important for the positive health effects associated with intake of beverages based on green tea.<sup>1,2</sup> The green tea polyphenols are antioxidants and have been found to be active through radical scavenging by electron transfer and hydrogen-atom transfer<sup>3,4</sup> and by radical addition followed by molecular rearrangements.<sup>5</sup> Green tea polyphenols are water-soluble, and their interaction with lipophilic antioxidants such as the tocopherols seems to be important for their protection of lipids and membranes against oxidative stress.<sup>6–8</sup> The green tea polyphenols are among the most reducing plant polyphenols and are more reducing than  $\alpha$ -tocopherol.<sup>9</sup> Accordingly, green tea polyphenols should be capable of regenerating  $\alpha$ -tocopherol from the  $\alpha$ -tocopherol radical, resulting from scavenging of lipid-derived radicals, provided that molecular contact is established at a water/lipid interface.<sup>10</sup> Such regeneration of  $\alpha$ -tocopherol by the green tea polyphenols has now been established in several studies.<sup>6,7,11</sup> It was further concluded that EC, EGC, ECG, and EGCG each may have even higher activity in the regeneration of vitamin E than vitamin C.<sup>8</sup>

Effective antioxidative protection often depends on interaction between different types of antioxidants resulting in antioxidant

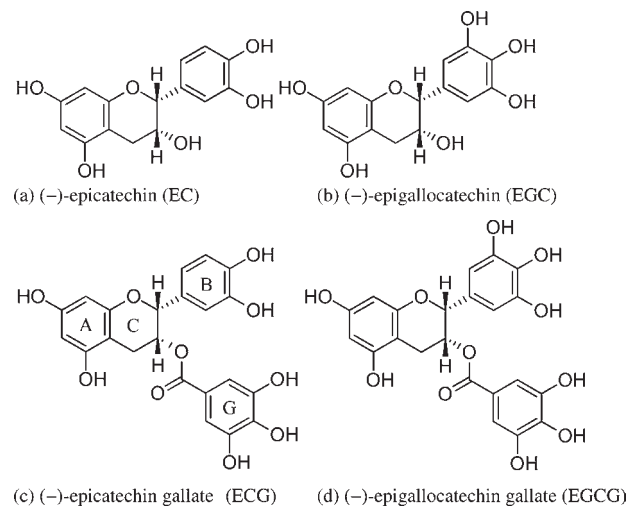


**Figure 1.** Molecular structures of (a) (–)-epicatechin (EC), (b) (–)-epigallocatechin (EGC), (c) (–)-epicatechin gallate (ECG), and (d) (–)-epigallocatechin gallate (EGCG). In (c) ring structures A, B, C, and G are indicated.

**Received:** July 28, 2011

**Revised:** October 24, 2011

**Accepted:** October 25, 2011

**Published:** October 25, 2011

synergism, as has been shown for  $\alpha$ -tocopherol/ascorbic acid, for  $\alpha$ -tocopherol/polyphenols, for carotenoids/polyphenols, and for  $\alpha$ -tocopherol/carotenoids.<sup>6,12,13</sup> Such antioxidant synergism is often the result of the regeneration of a chain-breaking antioxidant by another antioxidant less efficient under the actual conditions.<sup>14,15</sup> In contrast to many studies of interaction between  $\alpha$ -tocopherol and plant polyphenols such as the catechins<sup>6–8,11</sup> and between  $\alpha$ -tocopherol and carotenoids,<sup>13,14</sup> few studies have focused on carotenoid/polyphenol combinations.<sup>12,15</sup> Especially, the interaction between green tea polyphenols and carotenoids as antioxidants seems to have been neglected. It is not known whether the catechins may regenerate  $\beta$ -carotene ( $\beta$ -Car) as a lipophilic antioxidant, as seen for  $\alpha$ -tocopherol/catechin combinations.

The present study was accordingly designed to investigate catechins as antioxidants in liposomes as a membrane model in the presence and absence of  $\beta$ -Car combining a real-time kinetic study of free radical processes, which are of importance for such antioxidant interaction, and evaluation of antioxidant efficiencies of catechin/ $\beta$ -Car combinations in peroxidizing liposomes. Furthermore, quantum mechanical calculation combined with surface-enhanced Raman spectroscopy (SERS) was used to support the experimental findings to rationalize the differences between EC, EGC, ECG, and EGCG as antioxidants and between their respective interactions with  $\beta$ -Car and  $\alpha$ -tocopherol under oxidative stress. Notably, the results of these studies should also be of relevance for the tea industry, because black tea is produced from green tea leaves by the action of polyphenol oxidases, inherently present in tea leaves, resulting in oxidation of the catechins. During this process the carotenoids, also present in the tea leaves, are oxidatively cleaved to form important flavor components.<sup>16</sup>

## MATERIALS AND METHODS

**Chemicals and Sample Preparation.** EC (>90%), EGC (>95%), ECG (>98%), EGCG (>95%), gallic acid (GA, >97.5%), *all-trans*- $\beta$ -Car (>95%), soybean phospholipid mixture (1- $\alpha$ -phosphatidylcholine (PC) content  $\sim$  23%), 2,2'-azobis(2-methylpropionamide) dihydrochloride (AAPH, >97%), diammonium 2,2'-azinobis(3-ethylbenzothiazoline-6-sulfonate) (ABTS, 10 mg of substrate per tablet), and tetramethylammonium hydroxide (>97%) were purchased from Sigma-Aldrich (St. Louis, MO). 2,2'-Azobis(2,4-dimethylvaleronitrile) (AMVN, >95%) was purchased from Wako Pure Chemical Industries Ltd. (Osaka, Japan). Sodium dihydrogen phosphate, disodium hydrogen phosphate, potassium persulfate, silver nitrate, and sodium citrate (AR) were purchased from Beijing Chemical Works (Beijing, China). Methanol (HPLC grade, Fisher Scientific Inc., Waltham, MA) and ethanol (AR, Beijing Chemical Works) were used as received, whereas chloroform (AR, Beijing Chemical Works) was purified by distillation before use. To increase the solubility in aqueous solution, all four green tea polyphenols predissolved in ethanol were added into ion-exchanged water from a Milli-Q Academic water purification system (Millipore Corp., Billerica, MA). For laser flash photolysis experiments, conjugated bases of all four green tea polyphenols in methanol/chloroform binary solvent (1:9 v/v) were prepared by adding 1 equiv of tetramethylammonium hydroxide.

**Steady-State Surface-Enhanced Raman Spectroscopies.** Silver nanoparticles were used as SERS substrate. Briefly, 36 mg of silver nitrate was dissolved with 200 mL of ion-exchanged water and heated to 98 °C with reflux. Sodium citrate (40 mg) dissolved in 4.0 mL of ion-exchanged water was added to the flask. The mixture was boiled for 40 min with reflux under vigorous stirring using a magnetic stirrer to minimize undesired aggregation of silver nanoparticles. The green tea

polyphenol samples predissolved in ethanol were mixed with silver nanoparticle suspension, and the pH was controlled at 1; the samples were kept in U-shaped capillaries. Radiation of 514 nm from a continuous wave argon ion laser with an operating power of 20 mW was used for Raman excitation. The SERS spectra were collected during 5 min at a spectral resolution of 2  $\text{cm}^{-1}$ .

**Trolox Equivalent Antioxidant Capacity (TEAC).** ABTS<sup>•+</sup> solution was prepared by dissolving 20 mg of ABTS in 5.0 mL of ion-exchanged water and subsequent oxidation with addition of 3.5 mg of potassium persulfate. The final concentrations of polyphenols and ABTS<sup>•+</sup> were 10 and 20–200  $\mu\text{M}$ , respectively. The reaction kinetics of scavenging ABTS<sup>•+</sup> were followed by monitoring its characteristic absorption at 734 nm ( $\epsilon_{734} = 1.5 \times 10^4 \text{ L mol}^{-1} \text{ cm}^{-1}$ ). The absorbance difference ( $\Delta A_{734}$ ) before and after reaction was plotted versus ABTS<sup>•+</sup> concentration  $c$  and was fitted to the relationship  $\Delta A_{734} = a(1 - e^{-bc})$ . The TEAC values of all four green tea polyphenols were then derived as  $\text{TEAC} = a/(\epsilon_{734} \times c_{\text{antioxidant}} \times 1.9)$ , where 1.9 was the antioxidant capacity of Trolox.<sup>17</sup>

**Antilipoxidation Activity and Synergistic/Antagonistic Interaction with  $\beta$ -Carotene.** Liposome was prepared following refs 18 and 19 with certain modifications. AAPH and AMVN were used as radical initiators in the aqueous and lipid phase, respectively. Briefly, soybean PC (0.75 mM) and/or  $\beta$ -Car (7.5  $\mu\text{M}$ ) in chloroform was mixed with methanol. AMVN (32 mM) in methanol was added when needed, and the volume ratio of chloroform and methanol was 2:1. Solvents were removed under reduced pressure (0.01 MPa) with protection by high-purity nitrogen by using a rotary evaporator at a bath temperature of <20 °C. Afterward, high-purity nitrogen was introduced to reestablish the atmospheric pressure. The flask was covered with aluminum foil and kept in an ice–water bath under vacuum for 1.5 h.

The lipid residues with or without  $\beta$ -Car were rehydrated with 0.01 M phosphate buffer solution (pH 7.4) under sonication, and then 25  $\mu\text{L}$  of an ethanol solution of polyphenols ( $3.0 \times 10^{-4} \text{ M}$ ) was added to 5.00 mL of liposome suspension, and the ethanol vehicle was 0.5% v/v. AAPH (20 mM) in phosphate buffer solution was added when needed. The preparation was passed through hydrophilic polyethersulfone membranes (200 nm pore size) 20 times using Acrodisc syringe filters (Pall Corp., East Hills, NY) and then incubated for 90 min under room temperature and reduced light and oxygen partial pressure. The final concentration of PC was 0.15 mM, and those of AMVN and AAPH were 3.2 and 0.4 mM, respectively. The final  $\beta$ -Car and/or polyphenol concentrations were 1% of the molar fractions of PC.

Following ref 20 the time evolution profiles of AMVN- or AAPH-induced lipid peroxidation were traced by the absorbance of conjugated diene at the characteristic wavelength of 234 nm. Three milliliters of the suspension kept in a sealed 1 cm quartz cuvette was thermostated at  $45 \pm 1.0$  °C using a water-flow type thermostat (Neslab RTE-100, Thermo Fisher Scientific Inc., Waltham, MA) during the measurements. Liposomal preparation without antioxidant was used as a reference. The induction period (IP, in min) was determined as the time elapsed to the intersection of the tangent of the propagation phase and that of the induction phase and was corrected by subtracting the IP of the reference. The interaction between polyphenol and  $\beta$ -Car with equal concentration was studied, and a synergistic effect could be confirmed when the relationship  $\text{IP}_{\text{polyphenol}+\beta\text{-Car}} > \text{IP}_{\text{polyphenol}} + \text{IP}_{\beta\text{-Car}}$  was satisfied.

**Laser Flash Photolysis.** The experimental setup has been described in detail elsewhere.<sup>21</sup> Briefly, the pump laser pulse with 7 ns duration at 532 nm was supplied by a Nd:YAG laser operated at a repetition rate of 10 Hz (Quanta-Ray Pro-Series, Spectra Physics Lasers Inc., Mountain View, CA), and the pulse energy to excite the sample was  $\sim$ 5.0 mJ.  $\beta$ -Carotene (56  $\mu\text{M}$ ) and green tea polyphenols or their monoanion (20–100  $\mu\text{M}$ ) dissolved in the methanol/chloroform binary solvent (1:9, v/v) were kept in quartz cuvettes (optical path length = 1 cm) and stirred by the use of a magnetic stirrer. Near-infrared

kinetics probed at 950 nm for  $\beta$ -carotene radical cation ( $\beta$ -Car $^{*+}$ ) was detected with an avalanched photodiode (model CS460, Hamamatsu Photonics, Hamamatsu, Japan) attached to a TriVista spectrograph (Princeton Instruments, Trenton, NJ), and the kinetics traces were stored and averaged with a digital storage oscilloscope (bandwidth 600 MHz; LeCroy WaveSurfer 64Xs, Chestnut Ridge, NY) connected to a personal computer. For kinetics analyses, the time evolution profiles of optical density change ( $\Delta OD$ ) upon pulsed excitation were fit to a three-exponential model function as previously described<sup>12</sup>

$$\Delta OD = -A_1 \exp(-k_1 t) + A_2 \exp(-k_2 t) + A_3 \exp(-k_3 t)$$

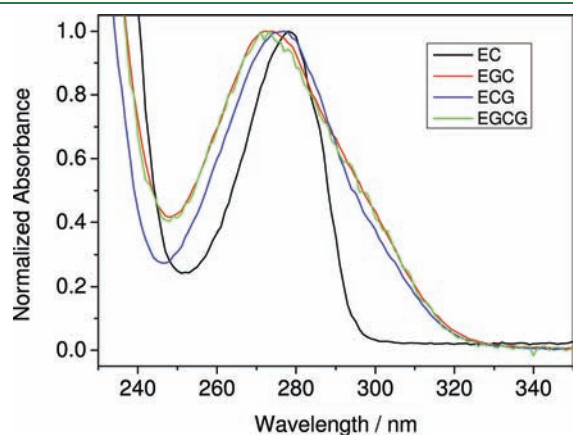


**Figure 2.** UV–visible absorption spectra of the green tea polyphenols in neutral aqueous solutions.

where  $A$  is the amplitude parameter and  $k$  is the pseudo-first-order rate constant. The program of least-squares curve fitting was coded on Matlab 5.3 (Mathworks Inc., Natick, MA), and the goodness of fitting was evaluated using  $\chi^2$  statistics.

**Quantum Chemical Calculations.** The molecular geometries of all four green tea polyphenols and their radicals and anions were optimized on the basis of the B3LYP density functional theory (DFT) in conjunction with the 6-31G(d,p) basis set by the use of the Gaussian 03 package.<sup>22</sup> Gas-phase bond dissociation enthalpy (BDE) and deprotonation enthalpy (DE) were calculated as the enthalpy difference of the processes  $\text{ArOH} \rightarrow \text{ArO}^{\bullet} + \text{H}^{\bullet}$  and  $\text{ArOH} \rightarrow \text{ArO}^- + \text{H}^+$ , respectively.<sup>15</sup> Relative intensities and frequencies of DFT-calculated Raman vibrational modes were corrected following refs.23–25.

## RESULTS

The four green tea polyphenols compared as antioxidants have an increasing number of phenolic groups from 4 to 8 (cf. Figure 1). The absorption maximum is shifted to lower wavelength for EGC and EGCG with *vicinal*-triphenol in the B-ring, whereas the galloyl moiety in ECG and EGCG rather increases the molar absorptivity (cf. Figure 2 and Table 1). Compared to the flavonoids and isoflavonoids, the catechins are in general more reducing but less acidic.<sup>26</sup> The reduction potential at pH 7.5<sup>9</sup> seems, however, not to depend on the number of phenolic groups,<sup>9</sup> but rather on the presence of *vicinal*-triphenol in the B-ring, making these catechins more reducing as seen from Table 1. EGC and EGCG, being more reducing, also have the weakest O–H phenolic bond among the catechins (lowest BDE), and this phenolic group for both EGC and EGCG is

**Table 1.** Molar Extinction Coefficients ( $\epsilon$  at  $\lambda_{\text{max}}$  Given), Calculated Dissociation Constants of Phenol Groups ( $\text{CpK}_a$  at 25 °C), Calculated and Experimental 1-Octanol/Water Distribution Coefficients (ClogD and logD at pH 7.4), Half-Wave Potential ( $E$ ), Trolox Equivalent Antioxidant Capacity (TEAC), Calculated Dipole Moments ( $\mu$ ), Calculated Lowest Bond Dissociation Enthalpy (BDE) and Deprotonation Enthalpy (DE) of Phenol Groups, and Energy (Gap) of Frontier Orbitals ( $E_{\text{HOMO}}$ ,  $E_{\text{LUMO}}$ , and  $\Delta E$ ) of Green Tea Polyphenols and Their Conjugated Bases

	EC	EGC	ECG	EGCG	
$\epsilon/\text{L mol}^{-1} \text{ cm}^{-1}$	$3.6 \times 10^3$ (278 nm)	$2.0 \times 10^3$ (272 nm)	$1.2 \times 10^4$ (277 nm)	$1.2 \times 10^4$ (273 nm)	
3 lowest $\text{CpK}_a^a$	9.00 (3'-OH)	8.73 (4'-OH)	8.03 (4''-OH)	7.99 (4''-OH)	
	9.62 (5-OH)	9.51 (5-OH)	8.90 (5-OH)	8.72 (4'-OH)	
	10.80 (4'-OH)	10.61 (3'-OH)	9.45 (3'-OH)	9.29 (5-OH)	
ClogD at pH 7.4 <sup>a</sup>	1.78	1.47	3.10	2.83	
logD at pH 7.4 <sup>b</sup>	0.30	-0.10	1.79	1.41	
$E/V$ vs NHE at pH 7.5 <sup>c</sup>	0.30	0.19	0.30	0.20	
TEAC at pH 7.4	3.64	5.44	4.50	5.41	
$\mu/\text{Debye}$	3.65	4.18	4.29	4.59	
lowest BDE/ $\text{kJ mol}^{-1}$	322.2 (4'-OH)	297.4 (4'-OH)	316.0 (4''-OH)	309.1 (4'-OH)	
lowest DE/ $\text{kJ mol}^{-1}$	1434.0 (3'-OH)	1425.9 (4'-OH)	1371.5 (4''-OH)	1372.6 (4''-OH)	
neutral	$E_{\text{HOMO}}/\text{eV}$	-5.68	-5.64	-5.62	-5.58
	$E_{\text{LUMO}}/\text{eV}$	0.03	0.14	-1.19	-1.16
	$\Delta E/\text{eV}$	5.71	5.78	4.43	4.42
monoanionic	$E_{\text{HOMO}}/\text{eV}$	-0.46	-0.37	-1.28	-1.29
	$E_{\text{LUMO}}/\text{eV}$	2.92	2.78	2.44	2.51
	$\Delta E/\text{eV}$	3.38	3.15	3.72	3.80

<sup>a</sup> Marvin Calculator Plugins were used for  $\text{pK}_a$  and logD calculations. Marvin 5.4.1, 2010, ChemAxon (<http://www.chemaxon.com>). <sup>b</sup> From ref 10. <sup>c</sup> from ref 9.

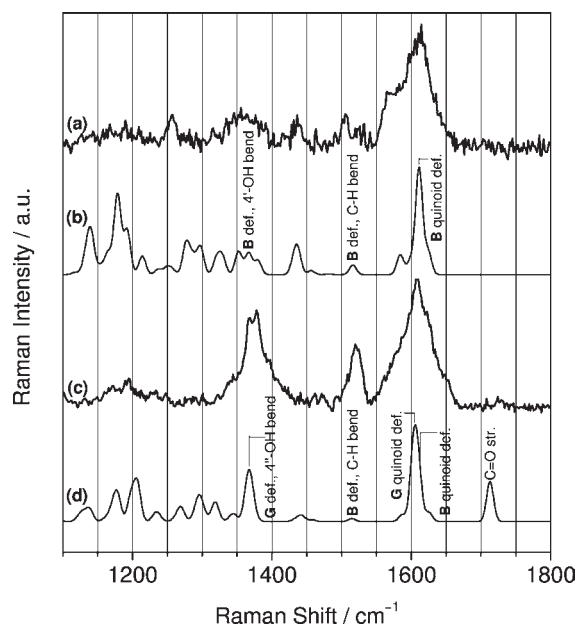


**Figure 3.** SERS and calculated Raman spectra of green tea polyphenols EC and ECG: (a) EC SERS; (b) EC calculated; (c) ECG SERS; (d) ECG calculated. For the assignments of vibrational modes, only those originated from the B- and G-rings are enhanced and indicated. See Table S2 in the Supporting Information for more detailed assignments.

located in the B-ring (4'-OH). In contrast to EGC and EGCG, EC has two phenol groups with comparable BDE values (Table 1 and Table S1 in the Supporting Information). Notably, only for ECG, the weakest O–H bond is found in the galloyl moiety. The most acidic phenolic group has been identified as the group with the lowest DE, and as may be seen from Table 1, the most acidic phenolic group is located in the B-ring for EC and EGC, whereas for ECG and EGCG with a galloyl moiety, the 4''-OH is more acidic. Only for EGCG are the most acidic phenolic group and the weakest O–H bond not located in the same ring.

The theoretical assessment of the most reducing phenolic group is proved by SERS spectroscopy using colloidal silver as the enhancement substrate. The vibrational modes in the vicinity of the adsorbing functionalities and those having the polarizability tensor components paralleling the normal of the substrate surface can be preferentially enhanced.<sup>27,28</sup> Figure 3 presents the SERS spectra of EC and ECG without and with the galloyl moiety, respectively. Among the phenolic groups that are helpful for the adsorption of flavonoids on the silver surface,<sup>29</sup> it is expected that those which have stronger reducing power interact more strongly with the silver surface, most likely via charge transfer resonance. It is seen from Figure 3a,b that the B-ring quinoid deformation at 1614  $\text{cm}^{-1}$  is enhanced significantly, whereas other vibrational modes remain rather weak. In the case of ECG (Figure 3c,d), the key Raman lines at 1378, 1520, and 1608  $\text{cm}^{-1}$  are preferentially enhanced. These observations strongly corroborate our theoretical evaluation that the 4'-OH on the B-ring and the 4''-OH of the galloyl moiety are most reducing in EC and ECG, respectively.

The energy gap of the frontier orbitals  $\Delta E$  as calculated from  $E_{\text{HOMO}}$  and  $E_{\text{LUMO}}$  does not correlate with the reduction potential for the catechins at pH 7.4. However, at this physiological pH, the catechins are partially dissociated according to the calculated  $\text{p}K_{\text{a}}$  values, which agree fairly well with the experimental values.<sup>3</sup> On the other hand, the energy gap for the

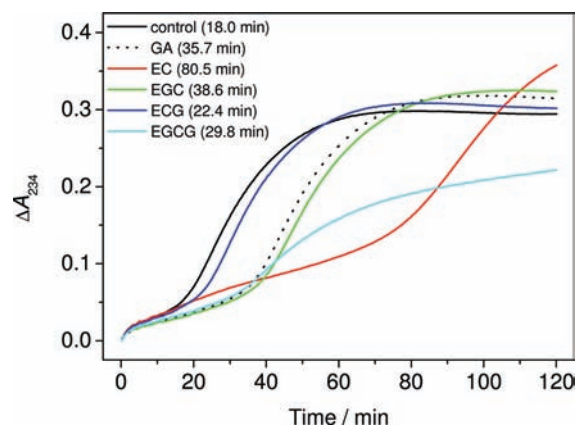


**Figure 4.** Time evaluation profiles of conjugated diene absorption at 234 nm arising from the lipoxidation initiated by AAPH in the aqueous phase in *L*- $\alpha$ -phosphatidylcholine (PC) liposome suspensions. Final concentrations:  $[\text{PC}] = 0.15 \text{ mM}$ ,  $[\text{AAPH}] = 0.4 \text{ mM}$ ,  $[\text{antioxidant}] = 1\%$  of PC molar fraction. Each curve is the average of three independent experiments. Lengths of induction period are indicated in parentheses in the legend.

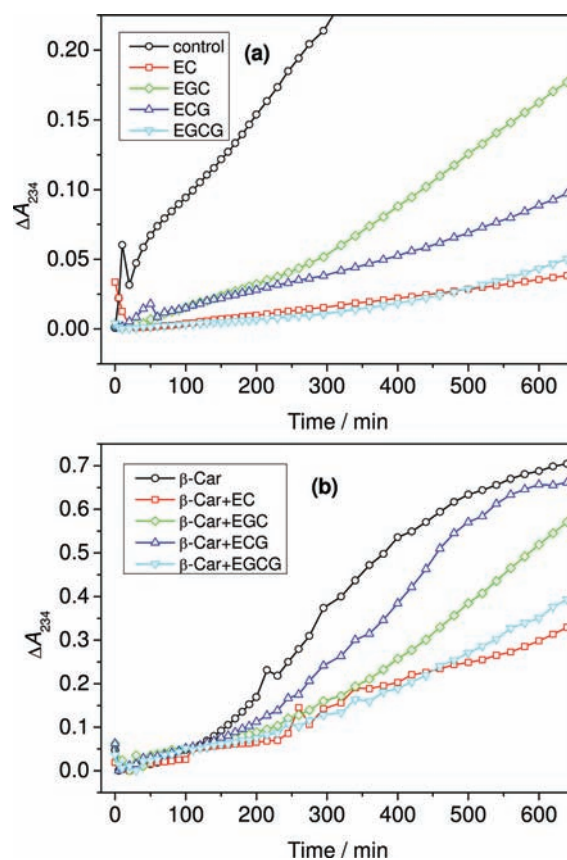


**Figure 5.** Time evaluation profiles of conjugated diene absorption at 234 nm arising from the lipoxidation initiated by AMVN inside liposome membranes in *L*- $\alpha$ -phosphatidylcholine (PC) liposomes without (a) or with (b)  $\beta$ -carotene added. Final concentrations:  $[\text{PC}] = 0.15 \text{ mM}$ ,  $[\text{AMVN}] = 3.2 \text{ mM}$ ,  $[\text{antioxidant}] = 1\%$  of PC molar fraction. Each curve is the average of three independent experiments.

monodeprotonated catechins calculated for the actual anion of the most acidic phenolic group in the individual catechins shows

no better correlation with reduction potentials at pH 7.4 (Table 1). The orbital energies and energy gaps calculated are all valid in the gas phase, and it seems that solvent effects are of at least equal importance for the redox properties as the actual orbital energies. The antioxidant capacity measured as TEAC showed a good correlation with the lowest BDE of the catechins as the same ordering EGC > EGCG > ECG > EC is seen for TEAC. Notably, TEAC does not simply depend on the number of phenolic groups present in the catechins or on the oxidation potential.

Besides the reduction potential and antioxidant capacity, the lipid/water distribution is expected to be important for antioxidant activity in heterogeneous systems such as membranes and liposomes. The 1-octanol/water distribution coefficients for pH 7.4<sup>10</sup> show a marked difference between the four green tea polyphenols, with ECG being the most lipophilic and EGC the most hydrophilic as is seen from the values in Table 1.<sup>10</sup> The *ClogD* values in Table 1 agree qualitatively with the experimental

**Table 2. Induction Periods (IP) Determined by Spectrophotometric Measurements of Conjugated Diene in Soybean PC Liposomes with or without  $\beta$ -Car with Free Radical Initiation by AMVN in the Lipid Phase and the Synergism between Green Tea Polyphenols and  $\beta$ -Car**

sample	IP/min		synergism/%
	without $\beta$ -Car	with $\beta$ -Car	
control	≈0	129.3	
EC	474.5	231.4	-61.7
EGC	308.6	305.1	-30.3
ECG	392.6	252.0	-51.7
EGCG	433.0	294.9	-47.6

values for incorporation of catechins into liposomes, for which the same ordering ECG > EGCG > EC > EGC has been reported.<sup>10</sup> EGC will, accordingly, mainly be located in the aqueous phase, whereas ECG will penetrate deepest into the lipid.

Lipid oxidation was initiated thermally in the aqueous phase of the liposomes using AAPH or in the lipid phase using AMVN. The progression of lipid oxidation was followed by spectrophotometric measurement of conjugated dienes as may be seen for the conditions with initiation in the aqueous phase in Figure 4 and in the lipid phase in Figure 5. For initiation of lipid oxidation in the aqueous phase, EC is clearly seen to be the most efficient antioxidant. From the length of the induction period (indicated in the legend in Figure 4), it may further be seen that gallic acid, included in part of the investigation, also delayed lipid oxidation. It should also be noted that there is no additivity for antioxidative effect in the comparison of the effects of gallic acid and EC added separately with ECG or of the effects of gallic acid and EGC added separately compared with EGCG. The ordering of antioxidative efficiency for initiation in the aqueous phase was EC  $\gg$  EGC > EGCG > ECG.

For lipid oxidation in the liposomes initiated in the lipid phase, EC was also found to be the most efficient antioxidant among the catechins with the following ordering: EC > EGCG > ECG > EGC.  $\beta$ -Car was added, and the efficiency of the catechins decreased and antioxidant synergism as previously defined

$$\text{antioxidantsynergism} = \frac{\text{IP}_{\beta\text{-car}+\text{catechin}} - (\text{IP}_{\beta\text{-car}} + \text{IP}_{\text{catechin}})}{\text{IP}_{\beta\text{-car}} + \text{IP}_{\text{catechin}}}$$

was in all cases negative, indicating antagonism (Table 2). The antagonistic effect is seen to be largest for the most efficient catechin as antioxidant and smallest for the least efficient (EC > ECG > EGCG > EGC).

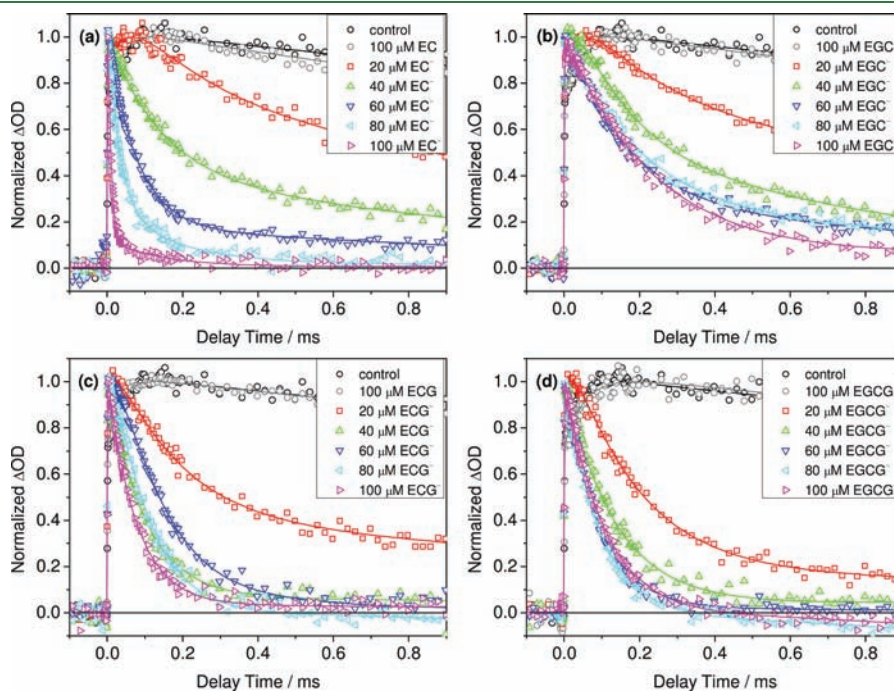


**Figure 6.** Decay kinetics of  $\beta$ -Car<sup>++</sup> ( $[\beta\text{-Car}] = 56 \mu\text{M}$ ) in methanol/chloroform (1:9, v/v) with the addition of neutral green tea polyphenols (100  $\mu\text{M}$ ) or their conjugated bases (20–100  $\mu\text{M}$ ). Samples: (a) EC; (b) EGC; (c) ECG; (d) EGCG. Excitation and detection wavelengths were 532 and 950 nm, respectively. Smooth lines are two- or three-exponential fitting curves. Each curve is the average of two independent experiments.

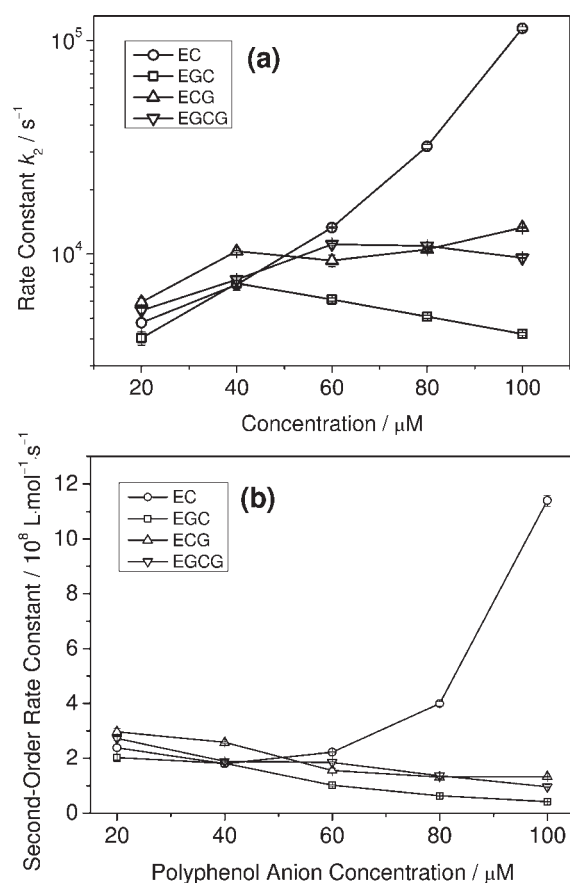


**Figure 7.** (a) Concentration dependencies of pseudo-first-order decay rate constants and (b) second-order decay rate constants of  $\beta\text{-Car}^{*+}$  with addition of green tea polyphenol anions.

## DISCUSSION

$\beta\text{-Car}$  is known to be a lipophilic antioxidant that effectively scavenges lipid-derived radicals through electron transfer and is regenerated by polyphenol anions or by tocopherols.<sup>13,30</sup> It is known, as a lipid-based antioxidant, to act synergistically with water-soluble polyphenolic antioxidants such as rutin and puerarin in liposomes for lipid oxidation processes initiated in the lipid phase.<sup>12,15</sup> The synergistic effect depends on a fast regeneration of  $\beta\text{-Car}$  as an efficient lipophilic antioxidant from  $\beta\text{-Car}^{*+}$ , the reaction product from reductive scavenging of lipid-derived radicals, by hydrophilic antioxidants, which are less effective as antioxidants under these conditions. The antioxidant synergism is kinetically controlled and depends on a proper contact in the lipid/water interface and on a fast electron transfer from the regenerating polyphenol anion to  $\beta\text{-Car}^{*+}$ .<sup>15</sup> The second-order rate constant for this bimolecular reaction between a carotenoid radical cation and a plant polyphenol has now been determined for several combinations of carotenoid and anions of plant polyphenols.<sup>30–32</sup>

The reaction between catechin anions and  $\beta\text{-Car}^{*+}$  was accordingly studied using laser flash photolysis with transient absorption detection.  $\beta\text{-Car}^{*+}$  was generated by photoexcitation (532 nm) in the electron-withdrawing methanol/chloroform (1:9 v/v) binary solvent. The formation and decay of  $\beta\text{-Car}^{*+}$  and the bleaching and regeneration of  $\beta\text{-Car}$  were followed at 950 and 500 nm, respectively, on a millisecond time scale in the absence or presence of each of catechin monoanions in

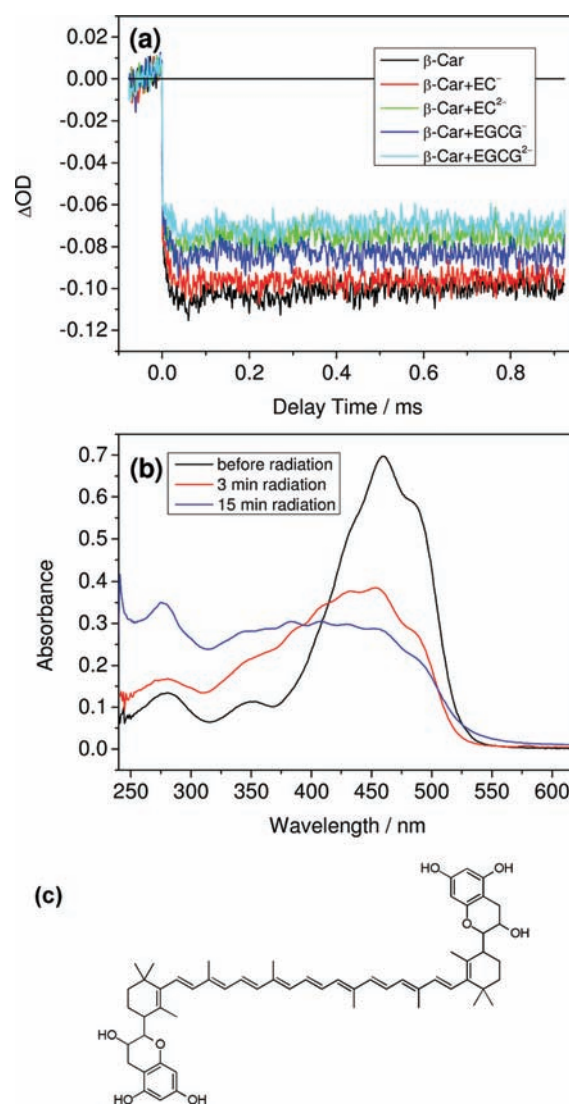


**Figure 8.** (a) Optical density change of  $\beta\text{-Car}$  ground state bleaching ( $[\beta\text{-Car}] = 56 \mu\text{M}$ ) in methanol/chloroform (1:9, v/v) with the addition of conjugated bases of EC and EGCG (60  $\mu\text{M}$ ). Excitation and detection wavelengths were 532 and 500 nm, respectively. Each curve is the average of two independent experiments. (b) Steady-state absorption spectra of EC (60  $\mu\text{M}$ ) and  $\beta\text{-Car}$  (56  $\mu\text{M}$ ) in methanol/chloroform (1:9 v/v) solution before and after laser radiation. (c) Speculative  $\beta\text{-Car}/\text{EC}$  adduct structure.

the 20–100  $\mu\text{M}$  concentration range. The decay of  $\beta\text{-Car}^{*+}$  was clearly accelerated by the presence of catechin anions but not by the neutral catechins, as is seen from Figure 6. The effect on decay is less significant than seen for anions of other polyphenols such as puerarin and daidzein.<sup>30</sup> The formation and decay of  $\beta\text{-Car}^{*+}$  could, however, be accounted for by a three-exponential expression (see Materials and Methods).

The formation of  $\beta\text{-Car}^{*+}$  corresponding to the first term was found to be a fast rising component and was almost independent of the nature of catechin present. The rate constants and amplitudes for the decay terms for the reaction between  $\beta\text{-Car}^{*+}$  and the catechin anion depend on the nature of the catechin and on the concentration of the catechin anion. In agreement with previous kinetic analyses, the fast decay component will be considered as the rate constant for the primary reaction between the catechin anion

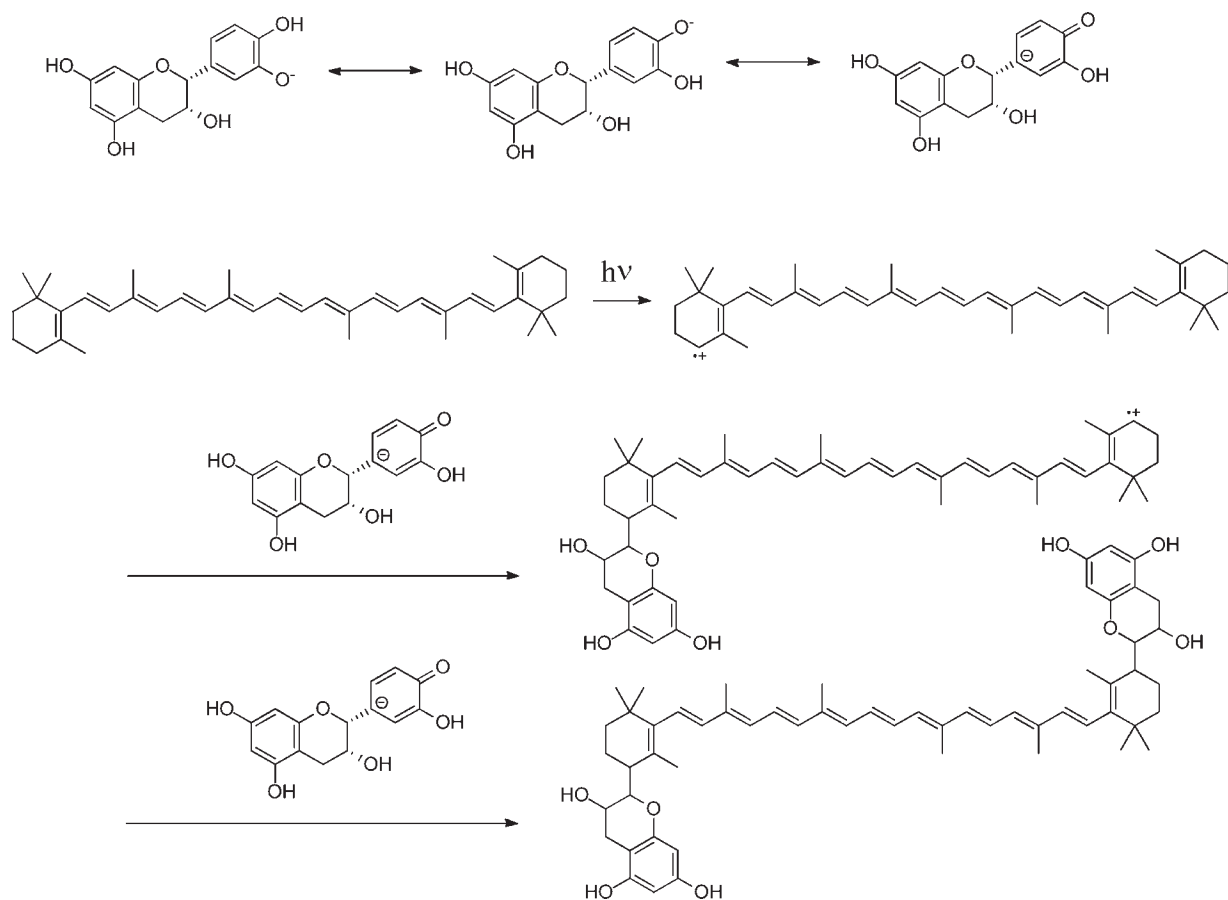
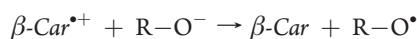
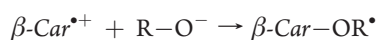


**Figure 9.** Schematic demonstration of speculative reaction mechanism between  $\beta$ -Car and EC.

and  $\beta$ -Car $^{\bullet+}$ .<sup>12,30</sup> The observed rate constants are pseudo-first-order and show a different dependence on the concentration of excess catechin anion as may be seen in Figure 7, where the pseudo-first-order and second-order rate constants are presented. The anion of EC, the most efficient of the catechins as an antioxidant, reacts with  $\beta$ -Car $^{\bullet+}$  with a rate approaching the diffusion limit for high catechin anion concentration. The different dependence for the rate constants on the concentration of excess catechin anion for the different catechins brought into question the validity of the simple electron transfer reaction known for other polyphenol anions:<sup>12,30</sup>



The bleaching of  $\beta$ -Car to yield the  $\beta$ -Car $^{\bullet+}$  was monitored at 500 nm in real time using laser flash photolysis with the same conditions. As is clearly seen from Figure 8a,  $\beta$ -Car is bleached, but is not regenerated in the presence of anions (or dianions) of catechins. Some other reaction between  $\beta$ -Car $^{\bullet+}$  and catechin anions may be responsible for the decay of  $\beta$ -Car $^{\bullet+}$ . As may be seen from Figure 8b, concomitant with bleaching of  $\beta$ -Car in the presence of a catechin anion, the  $\beta$ -Car absorption band is blue-shifted, which could indicate formation of an addition product of  $\beta$ -Car with less conjugation than  $\beta$ -Car:



The electron transfer is fast and depends on the driving force and approaches the diffusion limit for combinations of the most

reducing plant polyphenols and the most oxidizing carotenoid radical cations. A linear relationship was established between the activation free energy,  $\Delta G^\ddagger$ , and the reaction free energy,  $\Delta G^\circ$ , with a maximal rate for the reaction between astaxanthin radical cation and the puerarin dianion in methanol/chloroform (1:9 v/v) binary solvent.<sup>30</sup> The green tea polyphenols are among the most reducing plant polyphenols, and they have been demonstrated to protect  $\beta$ -Car against discoloration in foods.<sup>33</sup> An even more significant synergistic effect could accordingly be expected between carotenoids and the catechins as antioxidants. On the other hand, the driving force for electron transfer between green tea catechins and carotenoids may be too large, corresponding to an inverted region as known from the Marcus theory for electron transfer.<sup>34,35</sup> Clearly,  $\beta$ -Car is not regenerated by electron transfer by the green tea polyphenols despite this reaction according to the linear free energy relationship being predicted to be at the diffusion limit. The rate for the reaction between  $\beta$ -Car $^{\bullet+}$  and EC anion was found to approach the diffusion limit, but clearly in the transition state of the reaction, electron transfer becomes slower than formation of a carbon-carbon bond. A shift in reaction must be controlled by factors other than the driving force.

This suggestion was directly supported by mass spectroscopy (see the Supporting Information for LC-MS spectra). The reaction between  $\beta$ -Car $^{\bullet+}$  and EG or EGCG anion gave the same main reaction product with a molecular weight of 894.6 g mol<sup>-1</sup>. Tentatively, the reaction sequence of Figure 9 is suggested in which the C-4 radical cation, as the most

stable  $\beta$ -carotene radical, adds to the C-2 carbon of the polyphenol anion, because the C-2 position is partially negatively charged (see Figure S3 in the Supporting Information and refs 4, 31, and 32). The initially formed adduct, still being a radical cation, may subsequently react with a second polyphenol anion through the C-4' radical cation of the  $\beta$ -Car as part of the initially formed adduct. Although the reaction mechanism is still speculative, it explains the molecular mass of the adduct formed. In addition, the proposed structure of the main reaction product shown in Figure 8c can also account for the change of absorption spectra of the product with respect to the characteristic spectrum of  $\beta$ -Car; that is, the blue shift and the increased vibronic features can be explained by the presence of more isomeric  $\beta$ -Car/EC adduct forms as well as more severe twisting distortion compared to *all-trans*- $\beta$ -carotene. The different dependence on the catechin anion concentration noted for the decay of  $\beta$ -Car $^{*+}$  for the different catechins may be due to subsequent or parallel reaction involving elimination of the galloyl moiety from ECG and EGCG. Because  $\beta$ -Car as the efficient lipophilic antioxidant is not regenerated by the catechins, the expected synergistic effect in antilipoxidation for combination of catechins and  $\beta$ -Car is replaced by the significant antagonism seen for all four catechins investigated.

For lipid oxidation initiated both in the aqueous phase and in the lipid phase, EC is the most efficient antioxidant despite having the lowest number of the phenolic groups, the lowest TEAC value, and the highest value for the lowest BDE among the phenolic groups. A low dipole moment has been identified among flavonoids as an important microscopic property for antioxidative efficiency,<sup>36</sup> and EC has the lowest value for  $\mu$  among the four catechins (Table 1). To scavenge lipid-derived radicals, the catechin has to penetrate into the lipid bilayer. ECG, as the least effective antioxidant for initiation of oxidation in the lipid phase, has little, if any, contact with the lipid bilayer according to the distribution coefficient.<sup>10</sup> EGC and EGCG with the largest distribution coefficients seem to penetrate too deeply into the bilayer according to their lower efficacy as antioxidants for lipid oxidation initiated in the lipid phase. EGC and EGCG also have the largest value for  $\mu$ , and apparently in EC, a proper penetration into the lipid bilayer is combined with a low value for  $\mu$  to yield optimal function as antioxidant. Notably, this also results in the largest antagonistic effect for combinations of  $\beta$ -Car and catechins, because this also depends on reactions in the lipid bilayer between  $\beta$ -Car $^{*+}$  and the catechin.

In conclusion, the expected synergism between  $\beta$ -Car and the highly reducing green tea polyphenols as antioxidants in lipid/water heterogeneous systems with lipid oxidation initiated in the lipid phase was found to be replaced by a clear antagonism. The green tea polyphenols, rather than regenerating the lipophilic antioxidant  $\beta$ -Car from a radical cation, formed  $\beta$ -Car/catechin adducts. The appearance of adduct formation as an alternative reaction path to the electron transfer responsible for regeneration may be related to the very high exergonicity for electron transfer, corresponding to an "inverted region" in a rate/driving force profile. Two implications appear from the detection of this novel type of carotenoid–polyphenol adducts, both of which should be the subject of further studies. The first is related to the well-documented health effects of green tea. During oxidative stress, the green tea polyphenols will add to carotenoids and form compounds with higher lipophilicity, but still with the second, nonoxidized phenolic groups present for each catechin in effect transfer antioxidative capacity to the lipid phase. Other implications

relate to flavor formation in black tea, as these adducts may be intermediate in the oxidative degradation of carotenoids to form volatile molecules important for the flower notes of black tea infusions.

## ■ ASSOCIATED CONTENT

Supporting Information. Additional spectral information. This material is available free of charge via the Internet at <http://pubs.acs.org>.

## ■ AUTHOR INFORMATION

### Corresponding Author

\*E-mail: rliang06@ruc.edu.cn. Phone: +86-10-62516604. Fax: +86-10-62516444.

### Funding Sources

This work has been supported by the Natural Science Foundation of China (20803091) and the Research Funds for the Central Universities, and the Research Funds of Renmin University of China (RUC No. 10XNI007 and 42306063). L.H.S. is grateful for support from the Danish Research Council for Technology and Production as Grant 09-065906/FTP: Redox communication in the digestive tract.

## ■ ABBREVIATIONS USED

AAPH, 2,2'-azobis(2-methylpropionamide) dihydrochloride; ABTS, diammonium 2,2'-azinobis(3-ethylbenzothiazoline-6-sulfonate); AMVN, 2,2'-azobis(2,4-dimethylvaleronitrile);  $\beta$ -Car,  $\beta$ -carotene; BDE, bond dissociation enthalpy; DE, deprotonation enthalpy; DFT, density functional theory; EC, (–)-epicatechin; ECG, (–)-epicatechin gallate; EGC, (–)-epigallocatechin; EGCG, (–)-epigallocatechin gallate; GA, gallic acid; IP, induction period; LC-MS, liquid chromatography–mass spectroscopy; PC, L- $\alpha$ -phosphatidylcholine; SERS, surface-enhanced Raman spectroscopy; TEAC, Trolox equivalent antioxidant capacity.

## ■ REFERENCES

- (1) Graham, H. N. Green tea composition, consumption and polyphenol chemistry. *Prev. Med.* **1992**, *21*, 334–350.
- (2) Arab, L.; Liu, W.; Elashoff, D. Green and black tea consumption and risk of stroke. A meta-analysis. *Stroke* **2009**, *40*, 1786–1792.
- (3) Jovanovic, S.; Hara, Y.; Steenken, S.; Simic, M. G. Antioxidant potential of gallic catechins. A pulse radiolysis and laser photolysis study. *J. Am. Chem. Soc.* **1995**, *117*, 9881–9888.
- (4) Pedrielli, P.; Holkeri, L. M.; Skibsted, L. H. Antioxidant activity of (+)-catechin. Rate constant for hydrogen-atom to peroxy radicals. *Eur. Food Res. Technol.* **2001**, *213*, 405–408.
- (5) Valcic, S.; Muders, A.; Jacobsen, N. E.; Liebler, D. C.; Timmermann, B. N. Antioxidant chemistry of green tea catechins. Identification of products of the reaction of (–)-epigallocatechin gallate with peroxy radicals. *Chem. Res. Toxicol.* **1999**, *12*, 382–386.
- (6) Dai, F.; Chen, W.-F.; Zhou, B. Antioxidant synergism of green tea polyphenols with  $\alpha$ -tocopherol and L-ascorbic acid in SDS micelles. *Biochimie* **2008**, *90*, 1499–1505.
- (7) Zhou, B.; Wu, L.-M.; Yang, L.; Liu, Z.-L. Evidence for  $\alpha$ -tocopherol regeneration of green tea polyphenols in SDS micelles. *Free Radical Biol. Med.* **2005**, *38*, 78–84.
- (8) Mukai, K.; Mitani, S.; Ohara, K.; Nagaoka, S.-I. Structure-activity relationship of the tocopherol-regeneration reaction by catechins. *Free Radical Biol. Med.* **2005**, *38*, 1243–1256.



- (9) Yang, B.; Kotani, A.; Arai, K.; Kusi, F. Relationship of electrochemical oxidation of catechins on their antioxidant activity microsomal lipid peroxidation. *Chem. Pharm. Bull.* **2001**, *49*, 747–751.
- (10) Kajiya, K.; Kumazawa, S.; Nakayama, T. Steric effects of interaction of tea catechins with lipid bilayers. *Biosci., Biotechnol., Biochem.* **2001**, *65*, 2638–2643.
- (11) Pedrielli, P.; Skibsted, L. H. Antioxidant synergy and regeneration effect of quercetin, (–)-epicatechin and (+)-catechin on  $\alpha$ -tocopherol in homogeneous solutions of peroxidating methyl linoleate. *J. Agric. Food Chem.* **2002**, *50*, 7138–7144.
- (12) Liang, R.; Chen, C.-H.; Han, R.-M.; Zhang, J.-P.; Skibsted, L. H. Thermodynamic versus kinetic control of antioxidant synergism between  $\beta$ -carotene and (iso)flavonoids and their glycosides in liposomes. *J. Agric. Food Chem.* **2010**, *58*, 9221–9227.
- (13) Schroeder, M. T.; Becker, E. M.; Skibsted, L. H. Molecular mechanism of antioxidant synergism of tocotrienols and carotenoids in palm oil. *J. Agric. Food Chem.* **2006**, *54*, 3445–3453.
- (14) Tan, Y. S.; Webster, R. D. Electron-transfer reactions between the diamagnetic cation of  $\alpha$ -tocopherol (vitamin E) and  $\beta$ -carotene. *J. Phys. Chem. B* **2011**, *115*, 4244–4250.
- (15) Han, R.-M.; Tian, Y.-X.; Becker, E. M.; Andersen, M. L.; Zhang, J.-P.; Skibsted, L. H. Puerarin and conjugated bases as radical scavengers and antioxidants: molecular mechanism and synergism with  $\beta$ -carotene. *J. Agric. Food Chem.* **2007**, *55*, 2384–2391.
- (16) Berlitz, H. D.; Grosch, W.; Schieberle, P. *Food Chemistry*, 3rd ed.; Springer: Berlin, Germany, 2004; pp 239.
- (17) Arts, M. J. T. J.; Dallinga, J. S.; Voss, H. P.; Haenen, G. R. M. M.; Bast, A. A new approach to assess the total antioxidant capacity using the TEAC assay. *Food Chem.* **2004**, *88*, 567–570.
- (18) Hu, C.; Zhang, Y.; Kitts, D. D. Evaluation of antioxidant and prooxidant activities of bamboo *Phyllostachys nigra* Var. *Henonis* leaf extract in vitro. *J. Agric. Food Chem.* **2000**, *48*, 3170–3176.
- (19) Roberts, W. G.; Gordon, M. H. Determination of the total antioxidant activity of fruits and vegetables by a liposome assay. *J. Agric. Food Chem.* **2003**, *51*, 1486–1493.
- (20) Hwang, J.; Sevanian, A.; Hodis, H. N.; Ursini, F. Synergistic inhibition of LDL oxidation by phytoestrogens and ascorbic acid. *Free Radical Biol. Med.* **2000**, *29*, 79–89.
- (21) Han, R.-M.; Tian, Y.-X.; Wu, Y.-S.; Wang, P.; Ai, X.-C.; Zhang, J.-P.; Skibsted, L. H. Mechanism of radical cation formation from the excited states of zeaxanthin and astaxanthin in chloroform. *Photochem. Photobiol.* **2006**, *82*, 538–546.
- (22) Frisch, M. J.; Trucks, G. W.; Schlegel, H. B.; Scuseria, G. E.; Robb, M. A.; Cheeseman, J. R.; Montgomery, J. A., Jr.; Vreven, T.; Kudin, K. N.; Burant, J. C.; Millam, J. M.; Iyengar, S. S.; Tomasi, J.; Barone, V.; Mennucci, B.; Cossi, M.; Scalmani, G.; Rega, N.; Petersson, G. A.; Nakatsuji, H.; Hada, M.; Ehara, M.; Toyota, K.; Fukuda, R.; Hasegawa, J.; Ishida, M.; Nakajima, T.; Honda, Y.; Kitao, O.; Nakai, H.; Klene, M.; Li, X.; Knox, J. E.; Hratchian, H. P.; Cross, J. B.; Bakken, V.; Adamo, C.; Jaramillo, J.; Gomperts, R.; Stratmann, R. E.; Yazyev, O.; Austin, A. J.; Cammi, R.; Pomelli, C.; Ochterski, J. W.; Ayala, P. Y.; Morokuma, K.; Voth, G. A.; Salvador, P.; Dannenberg, J. J.; Zakrzewski, V. G.; Dapprich, S.; Daniels, A. D.; Strain, M. C.; Farkas, O.; Malick, D. K.; Rabuck, A. D.; Raghavachari, K.; Foresman, J. B.; Ortiz, J. V.; Cui, Q.; Baboul, A. G.; Clifford, S.; Cioslowski, J.; Stefanov, B. B.; Liu, G.; Liashenko, A.; Piskorz, P.; Komaromi, I.; Martin, R. L.; Fox, D. J.; Keith, T.; Al-Laham, M. A.; Peng, C. Y.; Nanayakkara, A.; Challacombe, M.; Gill, P. M. W.; Johnson, B.; Chen, W.; Wong, M. W.; Gonzalez, C.; Pople, J. A. *Gaussian 03W*, revision E.01: Gaussian Inc.: Pittsburgh, PA, 2003.
- (23) Yoshida, H.; Takeda, K.; Okamura, J.; Ehara, A.; Matsuura, H. A new approach to vibrational analysis of large molecules by density functional theory: wavenumber-linear scaling method. *J. Phys. Chem. A* **2002**, *106*, 3580–3586.
- (24) Scott, A. P.; Radom, L. Harmonic vibrational frequencies: an evaluation of Hartree–Fock, Moller–Plesset, quadratic configuration interaction, density functional theory, and semiempirical scale factors. *J. Phys. Chem.* **1996**, *100*, 16502–16513.
- (25) Polavarapu, P. L. Ab initio vibrational Raman and Raman optical activity spectra. *J. Phys. Chem.* **1990**, *94*, 8106–8112.
- (26) Han, R.-M.; Tian, Y.-X.; Liu, Y.; Chen, C.-H.; Ai, X.-C.; Zhang, J.-P.; Skibsted, L. H. Comparison between flavonoids and isoflavonoids as antioxidants. *J. Agric. Food Chem.* **2009**, *57*, 3780–3785.
- (27) Moskovits, M.; Suh, J. S. Surface selection rules for surface-enhanced Raman spectroscopy: calculation and application to the surface-enhanced Raman spectrum of phthalazine on silver. *J. Phys. Chem.* **1984**, *88*, 5526–5530.
- (28) Suh, J. S.; Moskovits, M. Surface-enhanced Raman spectroscopy of amino acids and nucleotide bases adsorbed on silver. *J. Am. Chem. Soc.* **1986**, *108*, 4711–4718.
- (29) Teslova, T.; Corredor, C.; Livingstone, R.; Spataru, T.; Birke, R. L.; Lombardi, J. R.; Canamares, M. V.; Leona, M. Raman and surface-enhanced Raman spectra of flavone and several hydroxyl derivatives. *J. Raman Spectrosc.* **2007**, *38*, 802–818.
- (30) Han, R.-M.; Chen, C.-H.; Tian, Y.-X.; Zhang, J.-P.; Skibsted, L. H. Fast regeneration of carotenoids from radical cations by isoflavonoid dianions: Importance of the carotenoid keto group for electron transfer. *J. Phys. Chem. A* **2010**, *114*, 126–132.
- (31) Guo, J.-J.; Hsieh, H.-Y.; Hu, C.-H. Chain-breaking activity of carotenes in lipid peroxidation: a theoretical study. *J. Phys. Chem. B* **2009**, *113*, 15699–15708.
- (32) Guo, J.-J.; Hu, C.-H. Mechanism of chain termination in lipid peroxidation by carotenes: a theoretical study. *J. Phys. Chem. B* **2010**, *114*, 16948–16958.
- (33) Unten, L.; Koketsu, M.; Kim, M. Antidiscoloration activity of green tea polyphenols on  $\beta$ -carotene. *J. Agric. Food Chem.* **1997**, *45*, 2009–2012.
- (34) Mayer, J. M. Simple Marcus-theory-type model for hydrogen-atom transfer/proton-coupled electron transfer. *J. Phys. Chem. Lett.* **2011**, *2*, 1481–1489.
- (35) Kojima, T.; Hanabusa, K.; Ohkubo, K.; Shiro, M.; Fukuzumi, S. Construction of  $\text{Sn}^{\text{IV}}$  porphyrin/trinuclear ruthenium cluster dyads linked by pyridine carboxylates: photoinduced electron transfer in the Marcus inverted region. *Chem.—Eur. J.* **2010**, *16*, 3646–3655.
- (36) Rasylev, B. F.; Abdullaev, N. D.; Syrov, V. N.; Leszczynski, J. A quantitative structure-activity relationship (QSAR) study of the antioxidant activity of flavonoids. *QSAR Comb. Sci.* **2005**, *24*, 1056–1065.